

X-Ray Detectors in Medical Imaging



Witold Skrzynski

1 Introduction

Various imaging modalities are used in medical imaging. In most of them, some kind of energy is emitted toward the patient. The energy interacts within the patient's tissues. The interaction leads to the creation of a signal that can be measured with detectors, usually placed outside the patient. If the measured signal is used to create an image, there is a need to map it to the location within the patient. To get a meaningful image, the measured characteristics of the signal have to differ depending on the type of the tissue or its state. Different modalities of medical imaging can show various characteristics of the tissue because they are based on various physical interactions. In ultrasonography, a mechanical wave with ultrasonic frequency is reflected by the tissues, which differ by acoustic impedance. In magnetic resonance imaging, an electromagnetic wave with radiofrequency gets absorbed by the tissues placed in a magnetic field and then is reemitted from the tissues. The intensity of reemitted wave depends on proton density and relaxation times. The wave's frequency depends on local magnetic field induction, allowing to separate signals from different locations.

Medical X-ray imaging is based on a measurement of the X-ray beam attenuation. The attenuation is different for different tissues and may be additionally modified by the presence of contrast agents (e.g., intravenously administered iodine) if needed. There are several X-ray modalities widely used in medicine. Depending on their application, they can utilize different energies of radiation (e.g., lower energy in mammography than in radiography), or a different method of image creation (radiography vs computed tomography), but the basic scheme is always

W. Skrzynski (✉)

Medical Physics Department, Maria Skłodowska-Curie National Research Institute of Oncology,
Warsaw, Poland

e-mail: witold.skrzynski@pib-nio.pl

kept: the patient is placed between a radiation source and radiation detector. The information from the detector is used to create an image.

2 Radiography

In the early days of X-ray imaging, glass plates with photographic emulsion were used as detectors, later replaced with films. The film is coated with a thin layer of photographic emulsion containing silver halide, which is not a very efficient X-ray absorber. The film performs much better in detecting visible light than X-rays. This is why the film has been quickly accompanied with an intensifying screen. The intensifying screen is a sheet of fluorescent material, converting the energy of each absorbed X-ray photon to many visible light photons. When the screen is in direct contact with the film, the film gets exposed by visible light. A combined screen-film detector has a much higher sensitivity for X-ray detection than the film alone. The sensitivity depends on the material used in the screen. As an example, screens with rare earth elements more effectively absorb and convert X-ray radiation compared to calcium tungstate screens (CaWO_4). With screen-film detectors, it is possible to obtain a radiographic image with a reasonably low patient dose. In medicine, the film is almost always used with intensifying screens, placed permanently in a light-tight radiographic cassette. In most cases, two screens are placed on both sides of the film, which has two layers of emulsion on both sides (Fig. 1a). The light emitted from the intensifying screen can penetrate the film base, reaching the second layer of emulsion and causing image blur. Compared with the film-only detector, the use of the screen-film decreases patient dose but at the cost of a lower spatial resolution of the image. Similarly, a film with larger silver halide grains is more sensitive but has a lower spatial resolution. In mammography, a good spatial resolution is essential for good visualization of microcalcifications, and only one intensifying screen and one layer of emulsion are usually used. In dental radiography, small objects are imaged, and a good spatial resolution is important, while radiation dose is not of much concern, and the film can be used alone [35].

Radiographic films require photochemical processing to convert latent images to visible images. It is a time-consuming process; it is not environmentally friendly and has to be done in the darkroom. Various alternatives have been proposed over the years. Some of them gained initial interest but then were practically forgotten due to low performance, high cost, or impracticality. As an example, the xeroradiographic detector consists of a plate covered with an amorphous selenium photoconductor. Before use, the surface of the plate is uniformly positively charged. During exposure, electrons are excited in the photoconductor, causing local loss of positive charge. After exposure, a negatively charged toner is applied. The toner is attracted to the residual positive charge on the plate, and then it can be moved to paper or plastic sheet, creating an image [39]. Interestingly, films that do not require photochemical processing and can be used in daylight conditions also exist. Radiochromic films become blackened directly by ionizing radiation, thanks to

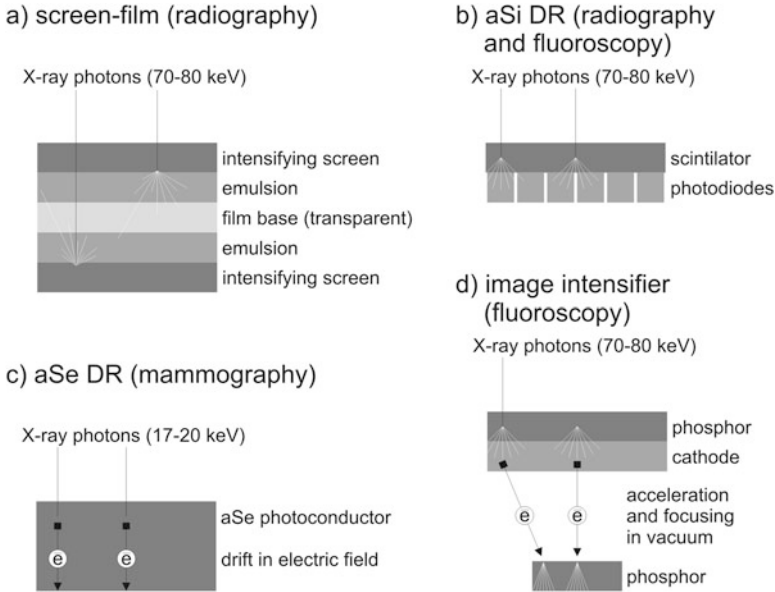


Fig. 1 Several detectors used in planar medical X-ray imaging (typical photon energies given for reference): **(a)** screen-film detector (radiography), **(b)** aSi detector (digital radiography), **(c)** aSe detector (digital mammography), **(d)** image intensifier (fluoroscopy).

radiation-induced polymerization of diacetylene (dark as polymer, colorless as a monomer). Radiochromic films are not sensitive enough to be used for imaging, but they may be used as radiation detectors to monitor skin doses in interventional radiology [9].

Modern radiography has largely moved away from film detectors toward digital imaging. Computed radiography (CR) imaging plates and digital radiography (DR) flat panel detectors do not need photochemical processing to get an image. They also have a much wider dynamic range than screen-film detector, e.g., $10^4:1$ instead of $10:1$ [8], and offer possibilities for digital processing, enhancement, and storage of the images.

In the CR systems, imaging plates are used as a radiation detector. The plate is placed in a radiographic cassette and emits visible light when absorbing X-ray radiation, which makes it similar to the intensifying screen in screen-film systems. At the same time, a sort of latent image is created on the plate, which makes it similar to film. During exposure, some electrons are trapped. During readout in the CR scanner, the imaging plate is illuminated with red laser, causing trapped electrons to relax to their ground state. The relaxation is associated with emission of blue light (photoluminescence), which is measured with a photomultiplier and used as an information to create an image. The light signal is proportional to the number of trapped electrons, which is in turn proportional to the received dose of radiation. Proper choice of storage phosphor materials for CR plates is essential

for good performance of the system. The efficiency of radiation-to-light conversion of the material is important, but other characteristics may be important as well. Some materials (e.g., CsBr:Eu²⁺) perform better than others (e.g., BaFX:Eu²⁺) because of their oriented, needlelike structure, which resembles a matrix of optical fibers. Such a structure reduces light scatter in the readout phase, thus resulting in less image blur even if the material layer is made thicker to achieve higher sensitivity [8].

In screen-film systems, the energy of the X-ray radiation is converted to the image with a time-consuming photochemical process. In CR systems, photochemical processing is not needed, but the plate is still a passive detector – it operates without any active means but does not provide a direct readout. Scanning of CR plates takes time; an image is available a few minutes after exposure. In DR flat panel detectors, the absorbed energy is converted to an electric charge within a detector, and the image is practically instantly displayed on the computer screen. In a vast majority of clinically used radiographic DR systems, the conversion is done with two steps, with intermediate conversion to light (Fig. 1b). First, X-ray radiation captured in a scintillation layer is converted to visible light. Second, the light is detected by a matrix of photodiodes. Electric charge is stored in a capacitor and then read out, amplified, digitized, and converted into an image. DR detectors with such indirect conversion are often referred to as aSi (amorphous silicon), although their amorphous silicon elements are not directly used in the detection of X-rays. This is done with the scintillation layer, which is made, e.g., of Gd₂O₂S or CsI. The materials differ in structure similarly as those used for CR imaging plates – while Gd₂O₂S is granular, CsI has a needlelike structure. Direct-conversion DR systems also exist and are often used in mammography. The energy of the absorbed X-ray radiation is converted directly to electrical charge within the amorphous selenium (a-Se) photoconductor (Fig. 1c). Electrons excited to the conduction band move along electrical field lines, without spreading to the sides, and are collected by the capacitors, similarly as in indirect DR detectors [32].

Not only detectors have evolved since the beginning of medical X-ray imaging history. Modern X-ray tubes are very different from those used in the first experiments: they have a higher vacuum, hot filament, line focus, proper shielding, higher filtration, usually rotating target, sometimes flat electron emitter, and a liquid bearing [6]. Tubes were constructed specifically for fluoroscopic/angiographic applications (long exposures, pulsed beam), mammography (lower voltage, smaller focal spot), and computed tomography (large g-force during rotation around a patient) [34]. Let the measure of improvement in the construction of X-ray radiation sources and detectors be a reduction in the average skin dose in pelvic radiographs: since 1896, it was reduced by a factor of about 400(!) [17].

3 Fluoroscopy

The screen-film detector integrates signals during whole exposure, which makes it suitable to capture an image of a stationary object. If the object moves, its image is blurred. Movements of the patient during imaging can be minimized with short exposure time and with immobilization. Patients can be asked to hold a breath, but it is not possible to stop internal movements such as heartbeat or peristalsis. In some situations, it is essential to visualize movements within a patient. Besides the movement of the patient's tissues, the flow of the contrast medium may be observed, movement of surgical instruments, or movement of implants, which are being placed in the patient. That is why a radiation detector is needed, which can provide a live view with a good time resolution.

In the early days of radiology, the live image was observed directly on the fluorescent screen. This resulted in large radiation exposure not only for the patient but also for the operator, who often kept the screen in hand. Since the image was not very bright, fluoroscopy could be only used in darkened rooms, which was inconvenient. In the 1950s, a new image detector for fluoroscopy was introduced, namely, X-ray image intensifier. The operation of the image intensifier consists of several steps. X-ray photons interact with a scintillation layer, converting each absorbed X-ray photon into many visible light photons (as with a simple fluorescent screen). The light strikes photocathode, knocking out electrons, which are then accelerated with electric potential and then fall again on another (smaller) fluorescent screen (Fig. 1d). As an effect, there are many more photons on the smaller screen, resulting in a much brighter (intensified) image with a smaller dose to a patient. The bright image can be observed in normal lighting conditions, recorded with a video camera, etc. Currently, image intensifiers are being replaced with flat panel (DR) detectors with a fast readout [2].

4 Tomographic Imaging

In radiography, three-dimensional structures are visualized in a two-dimensional planar image. The third dimension is lost in the imaging process. Images of objects located at different depths overlap, making some anatomical structures invisible. From the early days of medical X-ray imaging, researchers have tried to image selected planes within the patient [41]. Many experiments involved movement of the radiation source (tube) and/or detector (film) during the exposure. If the tube and detector are synchronously translated in opposite directions during exposure, only the objects located at one plane will be projected all the time at the same positions on the detector, resulting in a sharp image. For other objects, their projected image on the detector will move, resulting in blur. This idea was used in classical tomography (also called laminography) to obtain a sharp image of anatomical structures located at the focal plane (Fig. 2). Typically, only the image of one plane was obtained in

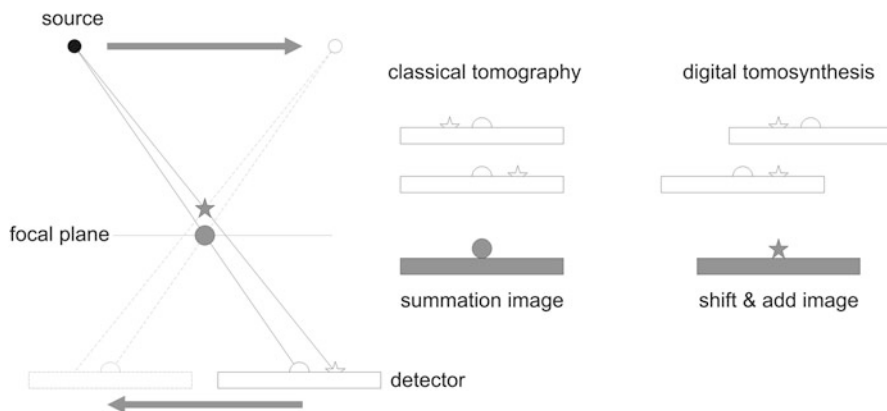


Fig. 2 Image acquisition in classical tomography (with film detector) and digital tomosynthesis (with flat panel DR detector)

one exposure. Another film and other exposure had to be used to image structures located on another plane. It was not only time-consuming but also associated with a multiplication of patient exposure. This limitation can be overcome quite easily if a different detector is used. If the film is replaced with a flat panel DR detector, tens of images at different angles can be acquired during the movement of the tube-detector system. If the images are simply summed up together, the same image as in classical tomography is obtained. If the images are shifted before summation, a different plane is sharply imaged. Thanks to an image detector with good time resolution and a very simple shift-and-add algorithm, images of several planes can be obtained from a single exposure. This solution, called digital tomosynthesis, is used clinically [22], although usually in a slightly different scheme (X-ray tube is moving over a segment of a circle, while the detector remains stationary).

Digital tomosynthesis is currently used mainly in breast imaging. Cross-sectional images of the head and body are usually obtained with X-ray computed tomography (CT). During the CT examination, tube and radiation detectors rotate around a patient, and a cross-sectional image is reconstructed with mathematical algorithms. Despite similarities between digital tomosynthesis and computed tomography, the geometry of the system is fundamentally different. In digital tomosynthesis, the image plane is perpendicular to the plane, in which the tube moves. In computed tomography, the image lays in the tube rotation plane.

In current multislice CT systems, there may be several rows of detectors (e.g., 64 rows with ca. 1000 detectors in each row). Detectors may perform two to three revolutions around a patient per second, registering the signal several hundred times during each rotation. Detectors for modern CT systems need not only to have good sensitivity and high dynamic range but also to be very fast and capable of working in large g-force conditions. For many years, xenon detectors have been used in CT, due to their good time characteristics (fast decay of signal). However, the low density of xenon – even pressurized – does not make it a very efficient detector for X-rays

[10]. Currently, CT detectors are usually made of scintillators and photodiodes [34]. The scintillators are chosen to have a high light output but also a low afterglow. The performance of the detectors, and thus also image quality, can be improved not only by choice of a better scintillator or more efficient photodiode but also by moving the analog-to-digital electronics as close as possible to the detectors, to minimize electronic noise [20].

5 Spectral Imaging

Attenuation coefficients for X-rays depend on the energy of photons. This dependence is different for different materials and tissues. This fact is used in bone densitometry (DXA, dual-energy X-ray absorptiometry), in which bone mineral density is calculated by comparing attenuation of radiation for two different energies [7, 23]. The typical radiographic image provides information about the attenuation of the radiation by the tissues, but it does not bring direct information about the density of the tissue. Identical attenuation can be observed e.g. for the thicker bone of lower density, as well as for thinner bone of higher density. In bone densitometry, quantitative information on bone density is calculated from absorption data measured for two different energies of radiation. Similar approach can be used to obtain other information. In contrast-enhanced spectral mammography, two exposures are made for two different beam energies (different tube voltage and different filtration). Both exposures are made after administration of an intravenous contrast agent, but detector data obtained for two energies may be processed to create virtual non-contrast image [29]. Possibility of using two energies to determine electron density and effective atomic number of the examined tissues has already been proposed for the first commercially available computed tomography system [31]. Currently, spectral CT allows for virtual monochromatic imaging, creation of virtual non-contrast images, better quantification of iodine content, and differentiation of renal stones based on their atomic composition [11, 15]. In some spectral computed tomography systems, the examination has to be performed twice to obtain data for two energies. Since the datasets are not obtained at the same time, patient movement can be an issue. Other spectral CT systems are capable of truly simultaneous imaging for two different energies, thanks to duplication of the tube-detector system or fast alternating tube voltage switching [13].

All the spectral imaging methods mentioned so far are based on the use of two radiation beams with two different energies. Another approach is also possible, based on a single beam, and provided that detector separately measures signals in two (or more) energy ranges. In one design of a spectral CT scanner, a layered detector is used, with two layers sensitive to two different energy ranges [13]. Another possibility is the use of photon-counting detectors (PCD), e.g., cadmium telluride semiconductors [21, 37]. The signal from most radiation detectors used in medical X-ray imaging is simply proportional to the total absorbed energy of radiation. In PCD, each detected X-ray photon generates a separately measured

electrical pulse. The height of each pulse can be compared with the threshold, or several different thresholds, to assign it to one of the energy bins. For each pixel, PCD provides information on the number of pulses separately for each energy bin. This allows for truly simultaneous acquisition of separate images for several energy ranges during one exposure. If several contrast agents are administered to a patient before an examination, with different radiation absorption characteristics (e.g., iodine and gadolinium), the virtual reconstruction of images with individual contrast agents is possible. Besides energy-resolving capabilities, photon-counting detectors have no electronic noise, which allows better imaging [3, 20].

6 Imaging at the Higher Energy of X-Ray Photons

In diagnostic X-ray imaging, the energy of X-ray radiation is optimized to achieve good visibility of anatomical structures with patient dose as low as possible. Depending on the application, tube voltage may be in the order of 25–35 kilovolts in mammography, several dozen kV in radiography and fluoroscopy, and up to 120–140 kV in computed tomography. This electric potential is used to accelerate electrons within the X-ray tube, and it sets a limit for the maximum energy of emitted photons (e.g., 140 keV in CT). Most of the photons reaching detectors have lower energy. However, imaging with photons of higher energy is also used in medicine.

In nuclear medicine imaging, a radioisotope is administered to the patient. After its uptake within the tissues, γ -radiation produced in the radioisotope's decay is detected from the outside of the patient. Tc-99m, which is the most widely used radioisotope for imaging, emits monochromatic γ quanta with an energy of 140 keV. In positron emission tomography (PET) imaging, a radioisotope is administered to the patient, which emits β^+ particles (positrons). Emitted positron annihilates with an electron, resulting in simultaneous emission of two 511 keV photons in opposed directions. Radiation detectors are distributed around the patient (Fig. 3a). If two of them coincidentally detect two photons, it is assumed that the photons originate from the same annihilation event. It is also assumed that the annihilation event has occurred on the line connecting the two detectors (LOR, line of response). This information is a base for image creation. Scintillators, which are used in PET as detectors, need to have a good time response with a very fast decay of light pulse to allow coincidence detection. They also need to have a good detection efficiency for 511 keV photons, which is usually associated with high density and high atomic number. Materials used in radiography (e.g., CsI, the density of 4.5 g/cm³) or computed tomography (e.g., CWO, the light decay time of 14.5 μ s) are not well suited for that task, compared to, e.g., LSO or LYSO scintillators (density 7–7.5 g/cm³, decay time ca. 40 ns) [26]. With a fast scintillator and a fast light detector (e.g., silicon photomultiplier), it is even possible to estimate time between detection of the two coincidence photons and to approximately determine the position of annihilation along the LOR. Inclusion of the additional data in image reconstruction

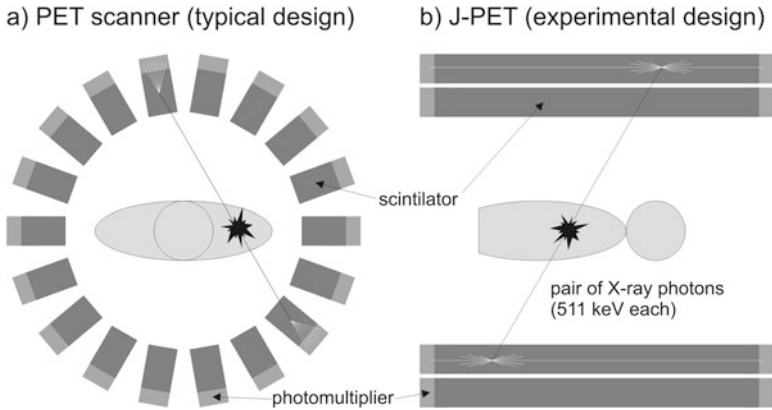


Fig. 3 Signal detection in positron emission tomography (PET) systems: (a) typical PET scanner design, (b) J-PET (experimental design)

improves image quality in the so-called time-of-flight (TOF) PET scanners [40]. Potentially, detectors with a much worse absorption efficiency could be also used in PET scanners. Compared to crystals commonly used in PET scanners, plastic scintillators have a low density (approximately 1 g/cm^3). Additionally, 511 keV photons usually do not leave all of their energy in the plastic scintillator during an interaction. However, the light pulse generated at each interaction is extremely short (1–2 ns), which allows us to obtain information on the place of interaction within the detector. Low-density plastic scintillator, used in a J-PET prototype in a non-typical geometrical setup (Fig. 3b), allows obtaining results comparable as for typical PET scanners [18, 24].

In oncology, radiotherapy with high-energy photon beams is used to treat patients with cancers. The maximum energy of photons in the therapeutic radiation beam is much higher in diagnostic radiology, with a typical value of 6 MeV. Although the beam is not optimized for imaging, it can be used for that task. The images obtained with the therapeutic beam (so-called portal images) can be used to verify the realization of the therapy, to check the alignment of the realized radiation field with a planned field and to verify the proper positioning of the patient. Originally, portal imaging was performed with films, and then various electronic portal imaging devices (EPIDs) were introduced. In one design, a fluorescent screen and a vidicon camera were used. The camera could not be placed directly on the beamline, because it would be hit with high-energy X-rays. Therefore, the light from the fluorescent screen was deflected with a mirror (Fig. 4a). In other designs, a matrix of liquid-filled ion chambers was used as the detector. An ion chamber filled with air, or even with a pressurized gas, would have a low detection efficiency for high-energy photons. Currently EPIDs are usually constructed similarly to radiographic flat panel DR detectors, with a scintillator layer and an array of photodiodes. The main difference between the DR detector and EPID is the presence of an additional metal layer (e.g., 1 mm of copper) in front of the scintillation layer (Fig. 4b).

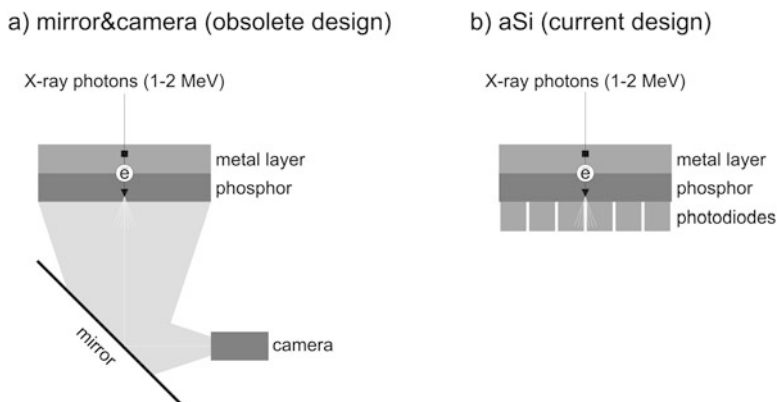


Fig. 4 Electronic portal imaging detectors (EPIDs) used in radiotherapy with high-energy X-ray photons (typical photon energies given for reference): (a) mirror and camera system (obsolete design), (b) aSi system (current design)

The metal layer is responsible for a generation of recoil electrons, which interact in the scintillator [1, 25, 42]. Additionally, detector elements (pixels) are usually significantly bigger in EPIDs than in radiography detectors (e.g., 400–800 μm vs 100 μm). Although bigger pixels lower detector's spatial resolution, such design allows each pixel to gather a higher signal in a shorter time.

7 Scattered Radiation

In traditional medical X-ray imaging, scattered photons add noise to an attenuation-based image. This is why in radiography anti-scatter grids are generally used, eliminating a large portion of the scattered photons. At the same time, an anti-scatter grid reduces the signal at the detector. That usually needs to be compensated with a higher patient dose compared to a no-grid setup. Other scatter-reduction methods include air gap, meaning the increased distance between patient and detector, and narrow beam geometry. If a narrow beam is used (pencil or slit), the trajectory of scattered photons will fall outside the beam and detector area. Slit-beam geometry is natural for CT scanners but may be also used in other imaging modalities, such as mammography [19].

In nuclear medicine imaging, monochromatic photons are used (radioisotope-emitted gamma rays). Detectors in gamma cameras can discriminate energy of each absorbed γ -ray quantum. A signal from scattered quanta, which has lower energy, can be eliminated with energy windowing, and only the monochromatic peak is used for image creation. That approach cannot be used in radiography. Even in the case of photon-counting detectors, the scattered photons cannot be separated over the wide spectrum of photons emitted from the X-ray tube. It could be possible if

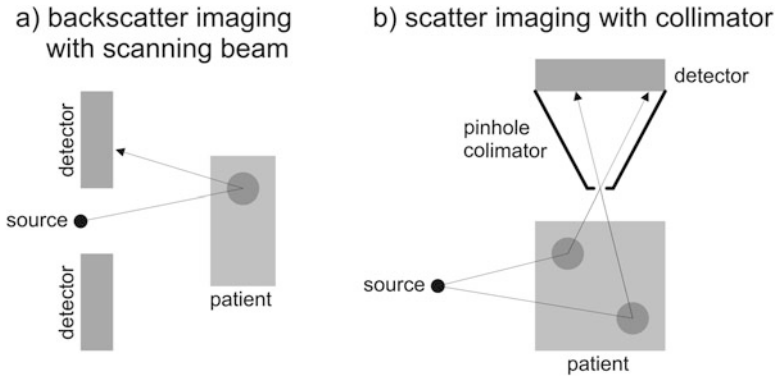


Fig. 5 Examples of scatter-based schemes for X-ray imaging: (a) backscatter imaging with scanning beam, (b) scatter imaging with collimator

a monochromatic beam was used, e.g., created with a conventional X-ray source combined with a mosaic crystal [12].

Photons, which are scattered in directions other than toward the detector, obviously do not have an impact on the quality of transmission image. While they are usually only of radiological protection concern, they could also be used for imaging. X-ray backscatter systems are used at many airports for passenger screening. Passenger, in a standing position, is scanned with a pencil radiation beam (Fig. 5a). Backscatter radiation is detected, allowing to image items hidden under clothes [16] with a low dose [36]. A similar scheme has also been considered for the imaging of humans [38]. A scanning beam has also been used to limit the volume, in which the radiation is scattered. If a large-area beam was used, the whole irradiated volume would be the source of scattered radiation, and it would be hard to distinguish between signals emitted by different organs. A similar situation can be observed in nuclear medicine imaging, where the whole patient is the source of radiation emitted by the radiopharmaceutical product present in his tissues. In nuclear medicine, this is solved by the use of slit collimators or pinhole collimators. This approach could be adapted to scatter-based imaging in lung radiotherapy (Fig. 5b). Lung tumor has a much higher density than the surrounding lung tissue and is a major source of radiation scatter. A slit X-ray kilovoltage beam may be used for imaging [43], as well as the megavoltage therapeutic beam itself [30]. Experiments show that scatter-based images may provide better tumor contrast as compared to transmission images obtained with EPID [30].

8 Forced Fluorescence

In the description of image formation in X-ray imaging, a photon that interacts through the photoelectric effect is referred to as removed from the beam. This is true

because such a photon transfers all of its energy to the electron. On the other side, a new X-ray photon may be emitted from the atom as a result of electron ejection (forced fluorescence). Human tissues are composed mainly of elements with a low atomic number, so the resulting monochromatic characteristic radiation has an energy of a few keV and does not reach the detector. The situation can change, if the patient is administered a contrast agent containing a high atomic number element, such as gold. The energy of characteristic radiation for gold is close to 70 keV. Theoretically, it is possible to create an image showing the capture of a contrast agent based on the registration of its forced fluorescence. In X-ray fluorescence computed tomography (XFCT), many detectors would be placed around the patient, and energy windowing and collimators with parallel holes would be used [5, 14]. Such fluorescence can be also caused by different beams, e.g., protons [4].

9 Phase-Contrast Imaging

In the above description, the X-ray beam was treated as a flux of particles (photons). At the same time, it can be described as a wave, with phase and trajectory changing while traveling through matter. The refraction of X-rays is much lower than the refraction of visible light, but it is observable. Possibility to obtain medical images dependent on refraction and phase change has been shown in experiments (phase-contrast imaging). One possibility is to pass the radiation coming from the patient through two gratings differing in spatial frequency [27]. As a result, we obtain a stronger or weaker signal not in the shadow of the entire structure but in places where the wave refracted on the patient's tissues. The image may appear similar to an attenuation-based X-ray image with an edge detection filter applied. In recent years, it has been shown that attenuation-based images and phase-contrast images of the mammary gland can be obtained simultaneously, during a several second exposure with a dose similar to regular mammography [33]. It has also been shown that phase-based mammographic images may be obtained at higher beam energies than traditionally used in mammography, with simultaneous improvement in lesion detectability and a patient dose saving compared to traditional attenuation-based imaging [28].

10 Summary

Various types of passive and active radiation detectors are used in medical imaging. In some of the active detectors, the energy of X-ray radiation is converted directly to electric charge and then to a digital image. In many systems, an intermediate conversion of the signal carriers takes place, e.g., to visible light. Different detector materials and designs can be chosen depending on the energy of radiation. The perfect detector could be characterized with high detection efficiency, high spatial,

time, and energy resolution. Usually, there is an interplay between the parameters, and depending on the application, one may want to, e.g., increase detector's sensitivity at the cost of its spatial resolution. While X-ray imaging in medicine is well-established, the availability of new detectors opens new possibilities. On the other hand, experimental imaging modalities create new possibilities for use of the existing radiation sources and detectors.

Bibliography

1. Baily, N. A., Horn, R. A., & Kampp, T. D. (1980). Fluoroscopic visualization of megavoltage therapeutic x ray beams. *International Journal of Radiation Oncology, Biology, Physics*, 6, 935–939. [https://doi.org/10.1016/0360-3016\(80\)90341-7](https://doi.org/10.1016/0360-3016(80)90341-7).
2. Balter, S. (2019). Fluoroscopic technology from 1895 to 2019 drivers: Physics and physiology. *Medical Physics International*, 7, 111–140.
3. Barber, W. C., Nygard, E., Iwanczyk, J. S., et al. (2009). *Characterization of a novel photon counting detector for clinical CT: Count rate, energy resolution, and noise performance*. In: Proceedings of SPIE.
4. Bazalova-Carter, M., Ahmad, M., Matsuura, T., et al. (2015). Proton-induced x-ray fluorescence CT imaging. *Medical Physics*, 42, 900–907. <https://doi.org/10.1118/1.4906169>.
5. Bazalova, M., Kuang, Y., Prax, G., & Xing, L. (2012). Investigation of X-ray fluorescence computed tomography (XFCT) and K-edge imaging. *IEEE Transactions on Medical Imaging*, 31, 1620–1627. <https://doi.org/10.1109/TMI.2012.2201165>.
6. Behling, R. (2018). X-ray tubes development- IOMP history of medical physics. *Medical Physics International*, 6, 8–55.
7. Cameron, J. R., & Sorenson, J. (1963). Measurement of bone mineral in vivo: An improved method. *Science*, 80(142), 230–232. <https://doi.org/10.1126/science.142.3589.230>.
8. Cowen, A. R., Davies, A. G., & Kengyelics, S. M. (2007). Advances in computed radiography systems and their physical imaging characteristics. *Clinical Radiology*, 62, 1132–1141. <https://doi.org/10.1016/j.crad.2007.07.009>.
9. delle Canne, S., Carosi, A., Bufacchi, A., et al. (2006). Use of GAFCHROMIC XR type R films for skin-dose measurements in interventional radiology. *Physica Medica*, 22, 105–110.
10. Fuchs, T., Kachelrie, M., & Kalender, W. A. (2000). Direct comparison of a xenon and a solid-state CT detector system: Measurements under working conditions. *IEEE Transactions on Medical Imaging*, 19, 941–948. <https://doi.org/10.1109/42.887841>.
11. Grajo, J. R., Patino, M., Prochowski, A., & Sahani, D. V. (2016). Dual energy CT in practice. *Applied Radiology*, 45, 61–62.
12. Green, F. H., Veale, M. C., Wilson, M. D., et al. (2016). Scatter free imaging for the improvement of breast cancer detection in mammography. *Physics in Medicine and Biology*, 61, 7246–7262. <https://doi.org/10.1088/0031-9155/61/20/7246>.
13. Johnson, T. R. C. (2012). Dual-energy CT: general principles. *AJR American Journal of Roentgenology*, 199, 3–8. <https://doi.org/10.2214/AJR.12.9116>.
14. Jones, B. L., & Cho, S. H. (2011). The feasibility of polychromatic cone-beam x-ray fluorescence computed tomography (XFCT) imaging of gold nanoparticle-loaded objects: A Monte Carlo study. *Physics in Medicine and Biology*, 56, 3719–3730. <https://doi.org/10.1088/0031-9155/56/12/017>.
15. Karçaaltuncaba, M., & Aktaş, A. (2011). Dual-energy CT revisited with multidetector CT: Review of principles and clinical applications. *Diagnostic and Interventional Radiology*, 17, 181–194. <https://doi.org/10.4261/1305-3825.DIR.3860-10.0>.
16. Kaufman, L., & Carlson, J. W. (2011). An evaluation of airport x-ray backscatter units based on image characteristics. *Journal of Transportation Security*, 4, 73–94. <https://doi.org/10.1007/s12198-010-0059-7>.

17. Kemerink, G. J., Kütterer, G., Kicken, P. J., et al. (2019). The skin dose of pelvic radiographs since 1896. *Insights Into Imaging*, *10*(39). <https://doi.org/10.1186/s13244-019-0710-1>.
18. Kowalski, P., Wiślicki, W., Shopa, R. Y., et al. (2018). Estimating the NEMA characteristics of the J-PET tomograph using the GATE package. *Physics in Medicine and Biology*, *63*. <https://doi.org/10.1088/1361-6560/aad29b>.
19. Lai, C. J., Shaw, C. C., Geiser, W., et al. (2008). Comparison of slot scanning digital mammography system with full-field digital mammography system. *Medical Physics*, *35*, 2339–2346. <https://doi.org/10.1118/1.2919768>.
20. Lell, M. M., Wildberger, J. E., Alkadhi, H., et al. (2015). Evolution in computed tomography: The battle for speed and dose. *Investigative Radiology*, *50*, 629–644. <https://doi.org/10.1097/RLI.0000000000000172>.
21. Leng, S., Bruesewitz, M., Tao, S., et al. (2019). Photon-counting detector CT: System design and clinical applications of an emerging technology. *Radiographics*, *39*, 729–743. <https://doi.org/10.1148/rg.2019180115>.
22. Machida, H., Yuhara, T., Tamura, M., et al. (2016). Whole-body clinical applications of digital tomosynthesis. *Radiographics*, *36*, 735–750. <https://doi.org/10.1148/rg.2016150184>.
23. Mazess, R. B., Peppler, W. W., & Gibbons, M. (1984). Total body composition by dual-photon (153Gd) absorptiometry. *The American Journal of Clinical Nutrition*, *40*, 834–839. <https://doi.org/10.1093/ajcn/40.4.834>.
24. Moskal, P., Rundel, O., Alfs, D., et al. (2016). Time resolution of the plastic scintillator strips with matrix photomultiplier readout for J-PET tomograph. *Physics in Medicine and Biology*, *61*, 2025–2047. <https://doi.org/10.1088/0031-9155/61/5/2025>.
25. Munro, P. (1995). Portal imaging technology: Past, present, and future. *Seminars in Radiation Oncology*, *5*, 115–133. [https://doi.org/10.1016/S1053-4296\(95\)80005-0](https://doi.org/10.1016/S1053-4296(95)80005-0).
26. Nassalski, A., Kapusta, M., Batsch, T., et al. (2007). Comparative study of scintillators for PET/CT detectors. *IEEE Transactions on Nuclear Science*, *54*, 3–10. <https://doi.org/10.1109/TNS.2006.890013>.
27. Olivo, A., & Speller, R. (2007). A coded-aperture technique allowing x-ray phase contrast imaging with conventional sources. *Applied Physics Letters*, *91*, 111–114. <https://doi.org/10.1063/1.2772193>.
28. Omoumi, F. H., Ghani, M. U., Wong, M. D., et al. (2020). The potential of utilizing mid-energy X-rays for in-line phase sensitive breast cancer imaging. *Biomedical Spectroscopy and Imaging*, 1–14. <https://doi.org/10.3233/BSI-200204>.
29. Patel, B. K., Lobbess, M. B. I., & Lewin, J. (2018). Contrast enhanced spectral mammography: A review. *Seminars in Ultrasound, CT, and MR*, *39*, 70–79. <https://doi.org/10.1053/j.sult.2017.08.005>.
30. Redler, G., Jones, K. C., Templeton, A., et al. (2018). Compton scatter imaging: A promising modality for image guidance in lung stereotactic body radiation therapy. *Medical Physics*, *45*, 1233–1240. <https://doi.org/10.1002/mp.12755>.
31. Rutherford, R., Pullan, B. R., & Isherwood, I. (1976). Measurement of effective atomic number and electron density using an EMI scanner. *Neuroradiology*, *11*, 15–21. <https://doi.org/10.1007/BF00327253>.
32. Samei, E., & Flynn, M. J. (2003). An experimental comparison of detector performance for direct and indirect digital radiography systems. *Medical Physics*, *30*, 608–622. <https://doi.org/10.1118/1.1561285>.
33. Scherer, K., Willer, K., Gromann, L., et al. (2015). Toward clinically compatible phase-contrast mammography. *PLoS One*, *10*, 6–12. <https://doi.org/10.1371/journal.pone.0130776>.
34. Shefer, E., Altman, A., Behling, R., et al. (2013). State of the art of CT detectors and sources: A literature review. *Current Radiology Reports*, *1*, 76–91. <https://doi.org/10.1007/s40134-012-0006-4>.
35. Sprawls, P. (2018). Film-screen radiography receptor development – A historic perspective. *Medical Physics International*, *6*, 56–81.
36. Stepusin, E. J., Maynard, M. R., O'Reilly, S. E., et al. (2017). Organ doses to airline passengers screened by X-ray backscatter imaging systems. *Radiation Research*, *187*, 229–240. <https://doi.org/10.1667/RR4516.1>.

37. Taguchi, K., & Iwanczyk, J. S. (2013). Vision 20/20: Single photon counting x-ray detectors in medical imaging. *Medical Physics*, *40*, 100901. <https://doi.org/10.1118/1.4820371>.
38. Towe, B. C., & Jacobs, A. M. (1981). X-ray backscatter imaging. *IEEE Transactions on Biomedical Engineering*, *BME-28*, 646–654. <https://doi.org/10.1109/TBME.1981.324755>.
39. Udoe, C. I., & Jafarzadeh, H. (2010). Xeroradiography: Stagnated after a promising beginning? A historical review. *European Journal of Dentistry*, *04*, 095–099. <https://doi.org/10.1055/s-0039-1697816>.
40. Vandenberghe, S., Mikhaylova, E., D'Hoe, E., et al. (2016). Recent developments in time-of-flight PET. *EJNMMI Physics*, *3*. <https://doi.org/10.1186/s40658-016-0138-3>.
41. Webb, S. (1992). Historical experiments predating commercially available computed tomography. *The British Journal of Radiology*, *65*, 835–837. <https://doi.org/10.1259/0007-1285-65-777-835>.
42. Woźniak, B., Ganowicz, M., Bekman, A., & Maniakowski, Z. (2005). A comparison of the dosimetric properties of the Electronic Portal Imaging Devices (EPIDs) LC250 and aS500. *Reports of Practical Oncology and Radiotherapy*, *10*, 249–254. [https://doi.org/10.1016/S1507-1367\(05\)71097-X](https://doi.org/10.1016/S1507-1367(05)71097-X).
43. Yan, H., Tian, Z., Shao, Y., et al. (2016). A new scheme for real-time high-contrast imaging in lung cancer radiotherapy: A proof-of-concept study. *Physics in Medicine and Biology*, *61*, 2372–2388. <https://doi.org/10.1088/0031-9155/61/6/2372>.